



**Citation:** S. Karayusufoğlu Uysal, L. Şaylan (2019) Assessment of Soil Heat Flux Equations for Different Crops under Semi Humid Conditions. *Italian Journal of Agrometeorology* (2): 49-61. doi: 10.13128/ijam-652

**Received:** June 25, 2019

**Accepted:** August 28, 2019

**Published:** October 29, 2019

**Copyright:** © 2019 S. Karayusufoğlu Uysal, L. Şaylan. This is an open access, peer-reviewed article published by Firenze University Press (<http://www.fupress.com/ijam>) and distributed under the terms of the Creative Commons Attribution License, which permits unrestricted use, distribution, and reproduction in any medium, provided the original author and source are credited.

**Data Availability Statement:** All relevant data are within the paper and its Supporting Information files.

**Competing Interests:** The Author(s) declare(s) no conflict of interest.

## Assessment of Soil Heat Flux Equations for Different Crops under Semi Humid Conditions

### Valutazione delle equazioni di flusso termico nel suolo per diverse colture in condizioni semi-umide

SEZEL KARAYUSUFOĞLU UYSAL<sup>1,\*</sup>, LEVENT ŞAYLAN<sup>2</sup>

<sup>1</sup> Turkish State Meteorological Service, Department of Weather Forecast, Remote Sensing Division, Ankara, Turkey

<sup>2</sup> Department of Meteorology, Faculty of Aeronautics and Astronautics, Istanbul Technical University, Istanbul, Turkey

\*Corresponding author email: [skarayusufoglu@mgm.gov.tr](mailto:skarayusufoglu@mgm.gov.tr)

**Abstract.** Soil heat flux (G) is an important component of energy balance by constraining the available amount of latent heat and sensible heat. There are many methods and formulations in the literature to estimate G accurately. In this study, widely used G estimation models are chosen to test. The models are based on Spectral Vegetation Indices (SVIs) namely, Normalized Difference Vegetation Index (NDVI), and Soil Adjusted Vegetation Index (SAVI) together with leaf area index (LAI), and crop height. Two successive growing periods of winter wheat (*Triticum Aestivum* L.), sunflower (*Helianthus annuus* L.), and maize (*Zea mays* L.) fields, located in the northwest part of Turkey, are used. Midday values (average of 09:30- 13:30) of G and net radiation ( $R_n$ ) used in order to capture the time period, when G is proven to be much dominant. According to the results, overall the best relation obtained with an exponential NDVI model with a determination coefficient value of 0.83 and a root mean square (RMS) error value of 20.28  $Wm^{-2}$  for maize. For winter wheat, G is predicted the best with SAVI based model ( $r^2=0.74$ ), and for sunflower, LAI based model worked best with 0.75  $r^2$  value. Crop height (CH) based nonlinear regression G model that suggested in this study worked better than linear models suggested in the literature with a better determination coefficient ( $r^2=0.70$ ) and a lower RMS error value (10.8  $Wm^{-2}$ ).

**Keywords.** Surface energy fluxes, Spectral Vegetation Indices, Bowen Ratio Energy Balance, Net Radiation.

**Abstract.** Il flusso termico nel suolo (G) è una componente importante del bilancio di energia capace di limitare la quantità disponibile di calore latente e calore sensibile. Ci sono molti metodi e formule in letteratura per stimare accuratamente G. In questo studio, i modelli di stima di G più utilizzati sono stati confrontati. I modelli sono basati sugli Indici di Vegetazione Spettrali (SVIs) chiamati Normalized Difference Vegetation Index (NDVI) e Soil Adjusted Vegetation Index (SAVI) insieme all'indice di area fogliare (LAI) e l'altezza della coltura. Due successivi cicli vegetativi del frumento (*Triticum Aestivum* L.), girasole (*Helianthus annuus* L.) e mais (*Zea mays* L.), coltivati

nella parte nordovest della Turchia, sono stati valutati. I valori presi a metà mattina (circa tra le ore 09:30-13:30) di G e radiazione netta ( $R_n$ ) sono stati usati al fine di cogliere il momento in cui G raggiunge i valori più elevati. In accordo con i risultati, la migliore relazione complessiva ottenuta è con il modello di NDVI esponenziale con un coefficiente di determinazione di 0.83 e un valore quadratico medio (RMS) di  $20.28 \text{ W m}^{-2}$  per il mais. Per il frumento, G è stato predetto meglio con il modello SAVI ( $r^2=0.74$ ) e per il girasole, il modello basato sul LAI ha funzionato meglio con un valore di  $0.75 \text{ r}^2$ . Il modello G di regressione non lineare basato sull'altezza della coltura (CH) proposto in questo studio ha lavorato meglio che il modello lineare suggerito in letteratura con un migliore coefficiente di determinazione ( $r^2=0.70$ ) e un più basso errore RMS ( $10.8 \text{ Wm}^{-2}$ ).

**Parole chiave.** Flussi di energia superficiale, Indici spettrali di vegetazione, Bowen Ratio Energy Balance, Radiazione netta.

---

## 1. INTRODUCTION

Soil (ground) heat flux (G), is known to be the smallest component of the earth's energy balance and widely assumed to be negligible. However, it has been proven that G is an essential component regarding land surface energy dynamics, especially during the daytime, almost for all ecosystems (Dugas *et al.*, 1996; Kustas *et al.*, 2000; Murray and Verhoef, 2007a). For a very well irrigated and fully covered vegetation surfaces, it is reported to be of the same order as sensible heat flux (H) (Kustas and Daughtry, 1990; Clothier *et al.*, 1986). For dry soil surfaces, G is as high as almost up to 50% (Idso *et al.*, 1975) and for forests, it is 30-50% of net radiation (Ogee *et al.*, 2001). In addition, for relatively sparse vegetation, G may grow into a meaningful component (Kustas *et al.*, 2000) and surpass others during the night (Murray and Verhoef, 2007a). Although occasionally neglected in daily evapotranspiration (ET) models, for much frequent ET estimations (e.g. 30 mins, hourly, etc.) and for sparse vegetation cover, G's contribution has been demonstrated to be significant (Kumar and Rao, 1984; Payero *et al.*, 2003, Payero *et al.*, 2005). Obtaining G, correctly, is crucial to understand the energy balance thoroughly.

Besides various measurement techniques, there are several methods to estimate G which depend on soil thermal properties and diurnal variation of soil surface temperature, weather data, and soil properties (e.g., Verhoef 2004; Murray and Verhoef 2007a and b; Núñez *et al.*, 2010; Verhoef *et al.*, 2012; Van der Tol 2012; Wang and Bras 1999; Hsieh *et al.* 2009). As an alternative, there are several empirical G estimation equations for different types of crops at different locations, in which remote sensing data involves (Choudhury *et al.*, 1987; Jackson *et al.*, 1985; Kustas and Daughtry, 1990; Kustas *et al.*, 1993; Boegh *et al.*, 2002, Tasumi, 2003).

Although it is not feasible to directly estimate G using satellite measurements, yet the ratio of G to another

component in the energy budget can be estimated (Kustas and Daughtry, 1990). For that, Jackson *et al.* (1985) suggested net radiation, because of its calculation ease with a minimum amount of meteorological data requirement.

Clothier *et al.* (1986) estimated the midday ratio of soil heat flux to net radiation ( $G/R_n$ ) as a linear function of a spectral vegetation index (near infrared to red ratio) over several regrowth cycles of alfalfa. Kustas and Daughtry (1990) demonstrated that multispectral data could provide a means of computing the  $G/R_n$  ratio for several cover types. Both studies showed that the  $G/R_n$  ratio linearly decreases with increasing vegetation cover and the multispectral vegetation indices.

$G/R_n$  ratio can be estimated close to the noontime via empirical relations from the leaf area index (LAI), normalized difference vegetation index (NDVI), soil adjusted vegetation index (SAVI), albedo ( $\alpha$ ), land-surface temperature (LST) that are obtained by satellites (Choudhury *et al.*, 1987; Bastiaanssen, 1995; Tasumi, 2003; Boegh *et al.*, 2002; Allen *et al.*, 2011).

Availability of data necessary to understand and analyse crop growth at field scale with a good temporal and spatial resolution and precision is possible with costly in situ measurements (Stroppiana *et al.*, 2006). Therefore, although being an indirect estimation technique, remote sensing is emphasized to be beneficial and useful considering areal scale assessments (Allen *et al.*, 2011). Even though micrometeorological measurement techniques such as Eddy Covariance provide much precise quantification, their spatial coverage and costs make remote sensing much preferable. For a thorough understanding of G, different types of crop-soil combinations are necessary to be studied. According to Turkish Statistical Institute's (TUIK) recent data (2017), within total cereal and other crops sown area (approximately 15.5 million ha), wheat has the greatest portion with about 8 million ha and around 21.5 million tonnes of total production. Maize is holding third place with about 640 000

ha cultivated area and almost 6 million tonnes of total production per year. Sunflower has the greatest portion off of the oilseeds with about 780 000 ha with a corresponding total production of around 195 000 tonnes per year. According to those mentioned information, wheat, sunflower, and maize are of great importance in terms of shaping the economy. Understanding and monitoring crops' growth by means of energy fluxes is almost an untouched topic for Turkey. Few studies are done and more needed to be carried out for better understanding.

Finally, the main purpose of this study is to test, optimize, and compare SVIs, LAI, and crop height-based empirical equations for G estimation and determine the best method for winter wheat, sunflower and maize. Additional aim is to assess and evaluate the relationships between  $G/R_n$  and biophysical factors such as biomass, crop height, and LAI.

## 2. MATERIALS AND METHOD

### 2.1 Study area

The study area is located in the Kırklareli city, in the north-western part of Turkey (41.69 N, 27.21 E). Experiments are conducted over winter wheat, sunflower and maize sown at Directorate of Atatürk Soil Water and Agricultural Meteorology Research Institute (AMRI) (Fig. 1).

Kırklareli city centre is 203 m above the mean sea level. On the north side of the city, Istranca Mountains lie in a northwest-southeast direction with the maximum elevation of approximately 1030 m at the southeast part (Fig. 2).

In a geographical information system (GIS) media, aspect and slope maps of the city generated from the

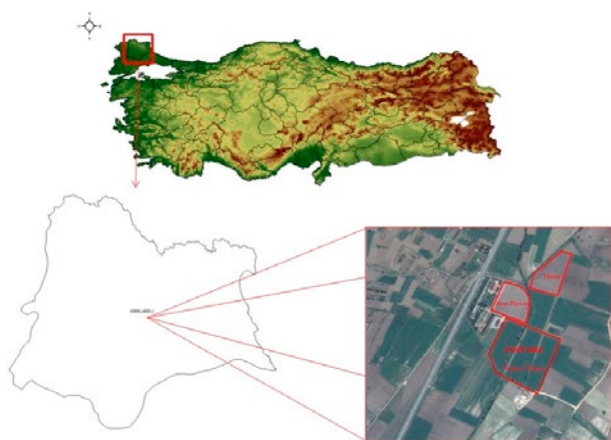


**Fig. 1.** Location of the study area.

**Fig. 1.** Posizione dell'area di studio.

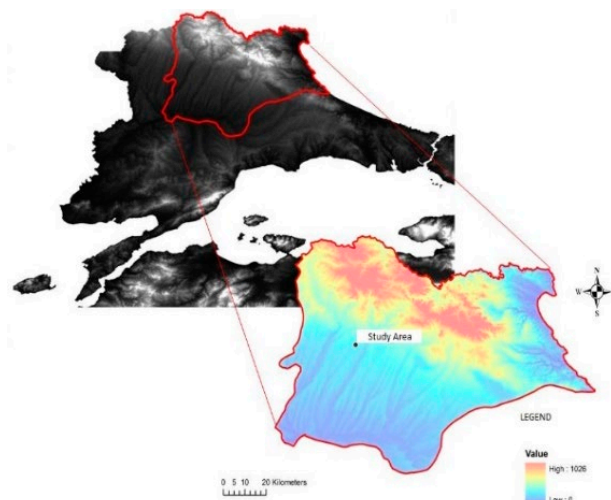


**Fig. 2.** Digital elevation map (DEM) of Kırklareli City (SRTM data).

**Fig. 2.** La mappa di elevazione digitale (DEM) della città di Kırklareli (SRTM dati).

digital elevation model (DEM). According to the results, the study area is oriented to the southeast with a 154° angle and ranked as a 0-2 class with 0.39-degree slope (Fig. 3).

### 2.2 Data used

#### 2.2.1. Meteorological and Soil Data

According to the long term mean monthly rainfall accumulations obtained from the Turkish State Meteorological Service (TSMS) from 1950 to 2014, the minimum amount of precipitation was observed in August (21.1 mm), and the maximum amount of precipitation was observed in December (70.6 mm). Besides, the mean annual accumulated rainfall amount for the study region is 573.6 mm. According to long term monthly temperature means, July is the warmest with 24°C whereas the coolest month was January (2.9°C). Extremes were also recorded in July for summer (42.5 °C on 27 July 2000) and in January for winter (-15.8 °C on 14 January 1972). As reported by the study conducted by TSMS's Climatology Branch (2000), Kırklareli city's climate has semi-humid properties with cool winters and warm summers as a shared output of well-accepted climate classification methods (Aydeniz, Erinç, De Martonne, Trewartha and Thornthwaite).

Automated weather observation systems settled in the planted area measured wind speed and direction, air temperature, relative humidity, global and net radiation, photosynthetic active radiation, surface tem-

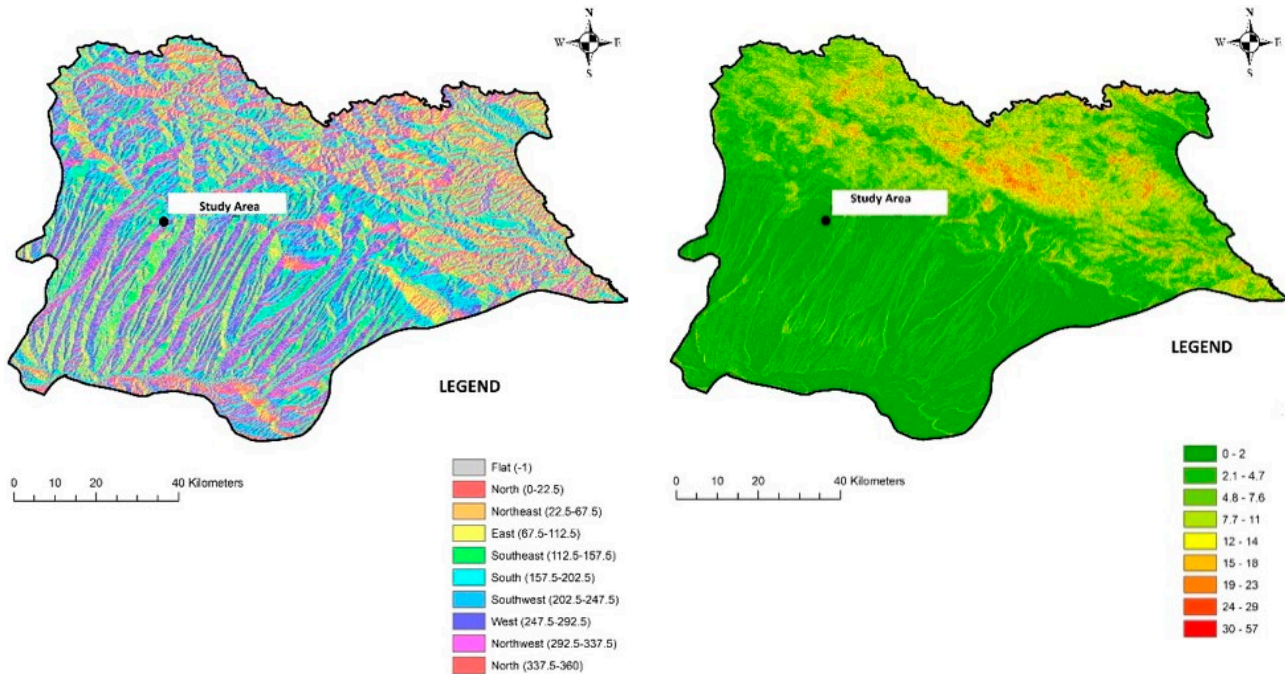


Fig. 3. Aspect and slope maps of Kırklareli City.

Fig. 3. Mapped di esposizione e pendenza della città di Kırklareli.

perature, heat fluxes, volumetric soil water content and rainfall amount during the growing periods (Şaylan et.al., 2010; Şaylan et.al 2018). Distribution of rainfall amount (mm), volumetric soil water content (%) for 0-30 and 30-60 cm of levels; soil temperature values at 2, 5, 10 and 20 cm depths for sunflower first and second growing periods (Fig. 4); for winter wheat's first and second growing periods (Fig. 5); and finally for maize first and second growing periods (Fig. 6) were demonstrated below.

According to the field studies, soil texture of wheat for 0-90 cm depth was 59 % sand, 25 % silt, and 16 % clay; for sunflower, 57 % sand, 20.8 % silt, and 22.2 % clay and finally for maize, 52.8 % sand, 16.7 % silt and 30.6 % clay. Considering FAO soil classification criteria the soil type of wheat area was sandy loam soil and it was sandy-clay loam for sunflower and maize fields.

### 2.2.2 Phenological Data

Phenological stages of winter wheat, sunflower and, maize observed and recorded during two sequential growing periods, and demonstrated in Fig. 7-9. For winter wheat, because less rainfall observed during the beginning of the second growing period, planting was done later than the first one. As a result, all phenological stages observed a few days later than the first period.

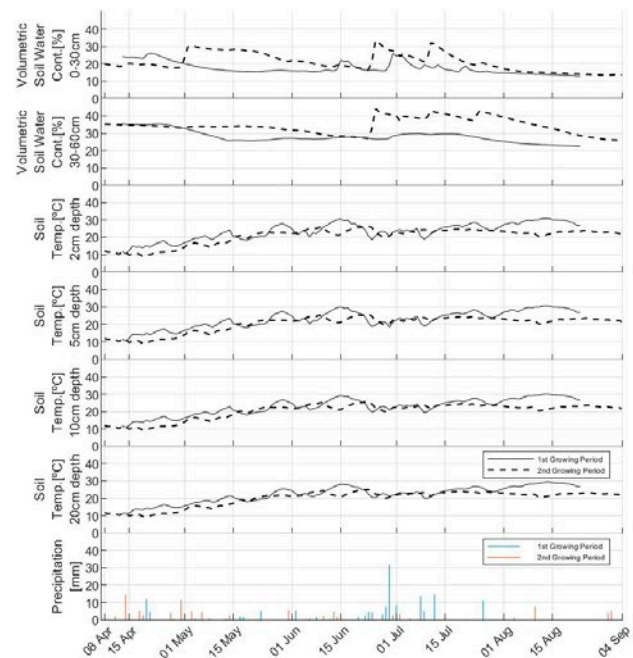
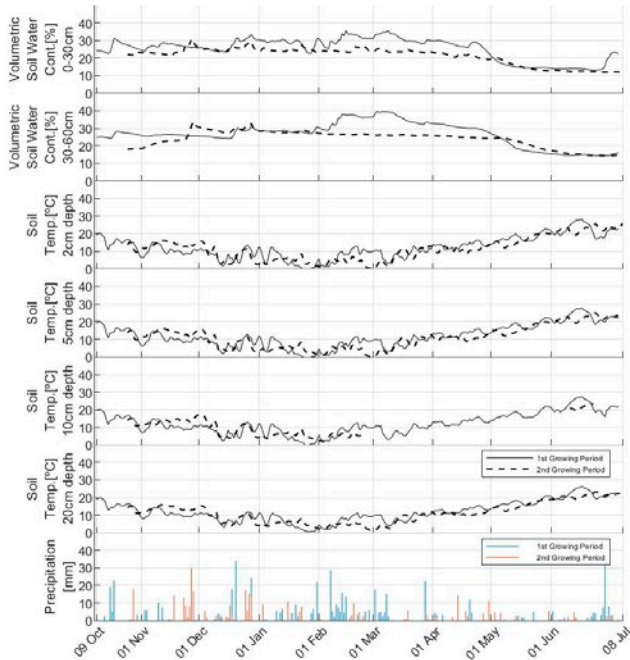
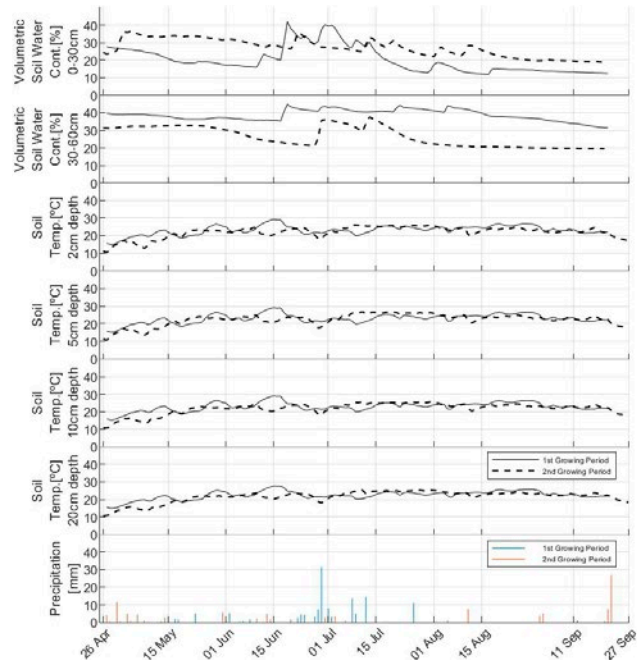


Fig. 4. Time series of volumetric soil water content, soil temperature, and precipitation, during both growing periods of sunflower.

Fig. 4. Serie temporale di umidità del suolo, temperatura del suolo e precipitazioni, durante entrambe le stagioni di crescita del girasole.



**Fig. 5.** Time series of volumetric soil water content, soil temperature, and precipitation, during both growing periods of winter wheat.  
**Fig. 5.** Serie temporale di umidità del suolo, temperatura del suolo e precipitazioni, durante entrambe le stagioni di crescita del frumento.



**Fig. 6.** Time series of volumetric soil water content, soil temperature, and precipitation, during both growing periods of maize.  
**Fig. 6.** Serie temporale di umidità del suolo, temperatura del suolo e precipitazioni, durante entrambe le stagioni di crescita del mais.

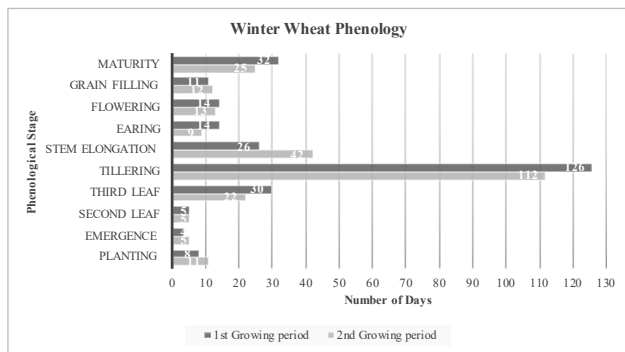


**Fig. 7.** Phenological stages of winter wheat for two growing periods.  
**Fig. 7.** Stadi fenologici del grano durante i 2 periodi di crescita.

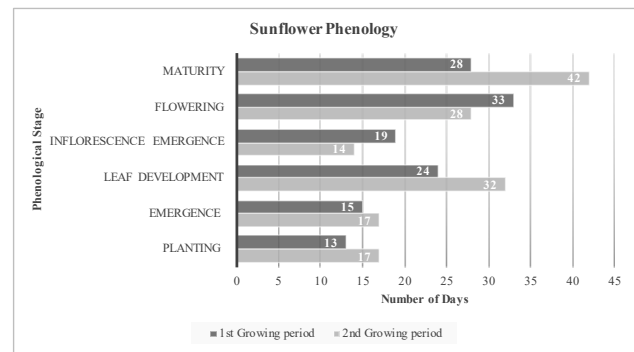


**Fig. 8.** Phenological stages of sunflower during two growing periods.  
**Fig. 8.** Stadi fenologici del girasole durante i 2 periodi di crescita.

Each crop field was fertilized by N fertilizer. Additionally, herbicide and fungicide treatments applied. Sunflower and maize irrigated but for winter wheat both seasons were without irrigation.

### 2.2.3 Spectral Reflectance Measurements

Each object has its unique reflectance pattern along the electromagnetic (EM) spectrum which is called spectral signature (Parker and Wolff, 1965). Spectral

signature has a key role in remote sensing in order to discriminate between objects. For instance, vegetation cover tends to absorb most of the incoming solar energy in visible (VIS) portion of the EM spectrum while it mainly reflects near-infrared (NIR) radiation incident upon it. Significant absorption in the VIS band is caused by the leaf pigments, namely because of the chlorophyll. Likewise, high reflection in the NIR band is a result of the cellular structure of the leaves (Basso *et al.*, 2001). Spectral vegetation indices (SVIs) have been

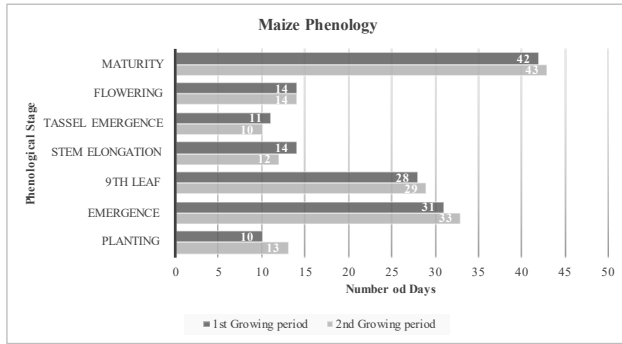


**Fig. 9.** Phenological stages of maize during two growing periods.  
**Fig. 9.** Stadi fenologici del mais durante i 2 periodi di crescita.

widely used for a better understanding of crop health and growth status by making use of that different behaviour of vegetation cover in VIS and NIR bands. In this study, spectral reflectance data measured with a hand type spectroradiometer (Fieldspec., ASD Inc.) which collects data in between 325-1075 nm. Measurements were done biweekly, under a clear and cloudless sky during both periods. SVIs that are shown in the below table calculated (Tab. 1).

**Tab. 1.** SVIs used in this study.

**Tab. 1.** SVIs usati in questo studio.

SVI	Equation	References
Normalized Difference Vegetation Index (NDVI)	$\frac{R_{(841-876)} - R_{(841-876)}}{R_{(841-876)} + R_{(841-876)}}$	Rouse <i>et al.</i> , 1974
Soil Adjusted Vegetation Index (SAVI)	$(1+L) * \frac{R_{841-876} - R_{620-670}}{R_{841-876} - R_{620-670} + L}$	Huete, 1988

Even though the measurements were done with spectroradiometer are not likely to be affected by atmospheric scattering, there is still a possibility of errors occurring because of technical or systematic issues of the instrument. Therefore, Savitzky-Golay (S-G) filtering was applied in order to reduce any noise that might be encountered. Although there were many SVIs calculated during the study, NDVI and SAVI were chosen to be investigated in terms of their capability to predict  $G/R_n$  ratio. NDVI and SAVI variation during both growing periods for maize, sunflower and winter wheat were demonstrated at Fig. 10 a,b.

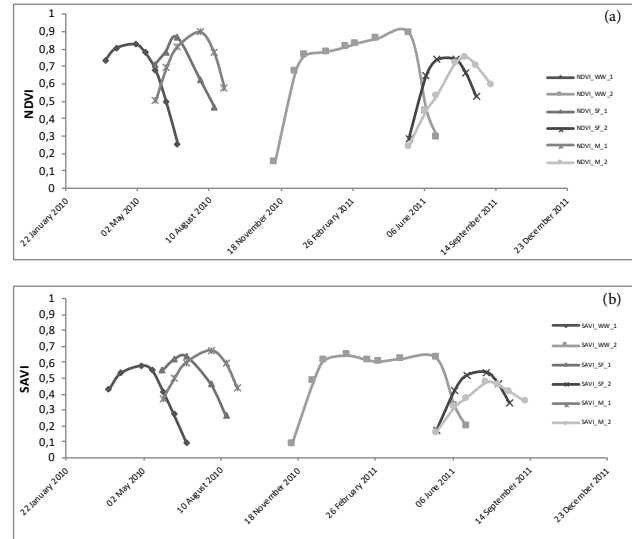


**Fig. 10.** (a) NDVI for first and second growing seasons (b) SAVI for first and second growing seasons for maize (M), sunflower (SF) and winter wheat (WW).

**Fig. 10.** (a) NDVI per il primo e secondo ciclo culturale (b) SAVI per il primo e secondo ciclo culturale per mais (M), girasole (SF) e frumento (WW).

## 2.2.4 Energy Budget Components

Net radiation and soil heat flux data measured and recorded during two growing periods for each crop with 10 and 30 min. intervals. Bowen Ratio Energy Balance (BREB) method was used in order to determine latent heat and sensible heat fluxes over crop's surfaces.

Before any further analysis carried out,  $R_n$  and  $G$  data sets were examined in terms of detecting any outliers and any missing values. Outliers detected using Interquartile Range (IQR) method, also called the Tukey method (Tukey, 1977) by which upper and lower limits determined by first and third quartiles of data sets. The data were filtered by Ohmura (1982) and Perez *et al.* (1999) criteria. Fig. 11 shows data after outliers removed by IQR (only sunflower data was demonstrated here).

As mentioned by other studies as well,  $G$  is highly affected by soil wetness as well as vegetation cover and surface temperature (Payero *et al.*, 2005; Kustas and Daughtry, 1990). Payero *et al.* (2005) and others (Camuffo and Bernardi, 1982; Novak, 1993; Domingo *et al.*, 2000) stated hysteresis problem with  $G$  data detected on the days after rain and irrigation. They reported that at the cases when wet soil starts to dry out, corresponding  $R_n$ - $G$  values differed dramatically compared to dry soil. In order to overcome this problem, the days with and after rain for wheat and the days with and after rain

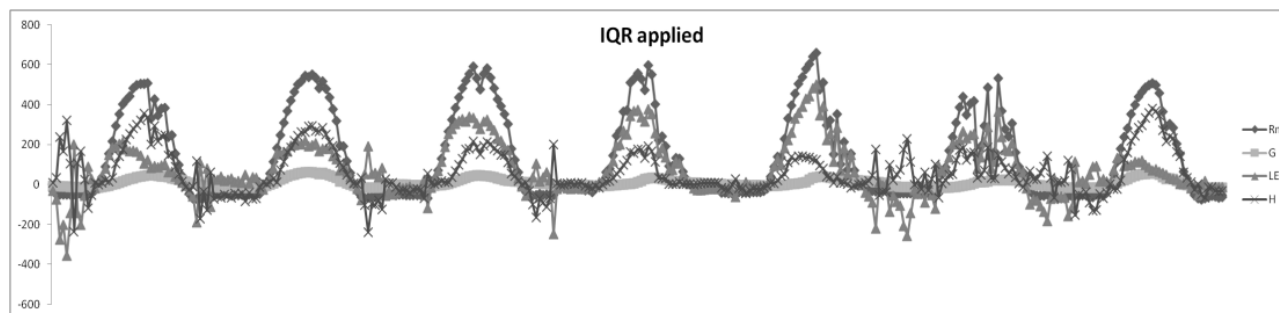


Fig. 11. Energy fluxes data after outliers cleared by IQR.

Fig. 11. Dati di flussi di energia dopo la eliminazione delle anomalie con IQR.

and irrigation for sunflower and maize, G and  $R_n$  data were removed from the data set.

In order to understand the apportionment of energy balance components during the day, 30 min. interval data sets for all three crops including two growing periods were used. According to data analysis, G data became dominant after 09:00 and got to its peak around 15:00 then came close to zero afterwards. Therefore 09:00-15:00 interval has been picked as daytime.

In order to make general analysis, after correction and elimination procedures completed, data were considered separately for each growing season. For winter wheat's first growing season G was 10% of  $R_n$  during daytime and at the second growing period, it was 15% of  $R_n$ , on average. The maximum value recorded for G was 100.4 W/m<sup>2</sup> and  $R_n$  was 769 W/m<sup>2</sup> for the first growing season and for the second growing season maximum value of G was 82.1 W/m<sup>2</sup> and maximum  $R_n$  value was 800 W/m<sup>2</sup>. For sunflower, at first growing season, G was 10% of  $R_n$  during the daytime, on average and 8% of  $R_n$  for the second growing period. The maximum value recorded for G and  $R_n$  were 93.6 W/m<sup>2</sup> and 794.3 W/m<sup>2</sup> for the first growing season and for the second growing season maximum values were 125.3 W/m<sup>2</sup> and 682.6 W/m<sup>2</sup>, respectively. For maize, at first growing season, G was 5% of  $R_n$  during the daytime, on average and 9% of  $R_n$  at the second growing period. The maximum value recorded for G was 131.4 W/m<sup>2</sup> and it was 692.7 W/m<sup>2</sup> for  $R_n$  at the first growing season. At the second growing season, maximum values for G and  $R_n$  were 131.4 W/m<sup>2</sup> and 692.7 W/m<sup>2</sup>, respectively.

G is highly dependent on surface conditions (i.e., wet or dry and bare or vegetated). For bare soil, G may be 20-50% of  $R_n$  depending on soil moisture (Idso *et al.*, 1975) whereas, for mature crops, G may be 5-10% of  $R_n$  over alfalfa (Clothier *et al.*, 1986), wheat (Choudhury *et al.*, 1987), and soybeans (Baldocchi *et al.*, 1985). Thus, soil heat flux can be a significant portion of  $R_n$  ranging

from 5% to 50% of  $R_n$  depending on soil moisture and fraction of vegetation cover.

In order to better capture G dominance, midday (09:30-13:30) 30 minutes interval average G/ $R_n$  values were examined for each crop considering their phenological stages (Tab. 2).

Although results for each crop were in line with the sense that G/ $R_n$  values decreasing with the growing plant, there were differences because of the differing soil moisture, surface temperature, soil content, weather conditions (e.g., precipitation, cloudiness).

Crop	Phenological Stage	1st Growing Season			2nd Growing Season		
		G/ $R_n$ Midday					
		Min	Ave	Max	Min	Ave	Max
Winter Wheat	Emergence-Tillering	0.12	0.26	0.58	0.07	0.13	0.23
	Stem Elongation-Earing	0.03	0.09	0.26	0.02	0.07	0.17
	Flowering-Maturity	0.03	0.07	0.08	0.02	0.04	0.06
	Maturity-Harvest	0.03	0.10	0.39	0.02	0.05	0.15
Sunflower	Emergence-Inflorescence	0.03	0.09	0.22	0.01	0.14	0.42
	Flowering-Maturity	0.03	0.10	0.16	0.01	0.08	0.21
	Maturity-Harvest	0.01	0.05	0.22	0.01	0.05	0.20
Maize	Emergence-Stem Elongation	0.01	0.08	0.22	0.06	0.18	0.33
	Tasselling-Flowering	0.03	0.07	0.34	0.05	0.10	0.19
	Flowering-Maturity	0.03	0.05	0.07	0.02	0.06	0.11
	Maturity-Harvest	0.03	0.05	0.07	0.04	0.07	0.33

### 3. RESULTS

#### 3.1 Relations between G/ $R_n$ and Biophysical Parameters

LAI of each crop was measured biweekly using a plant canopy analyzer (LAI-2000 sensor of LI-COR). Aboveground dry biomass was measured conventional-

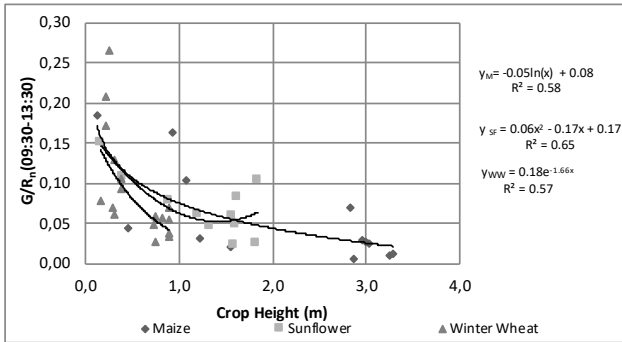


**Fig. 12.** Relationship between the ratio of  $G$  to  $R_n$  and crop height for winter wheat, sunflower, and maize.

**Fig. 12.** Relazione fra  $G$  e  $R_n$  e l'altezza della coltura in frumento, girasole e mais.

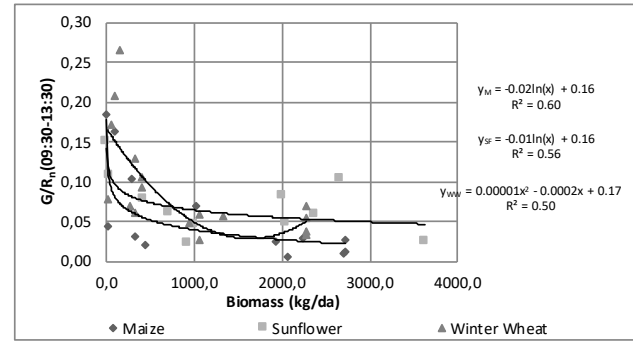


**Fig. 14.**  $G/R_n$ - biomass relationships for winter wheat, sunflower, and maize.

**Fig. 14.** Relazioni tra  $G/R_n$ - biomassa in frumento, girasole e mais.

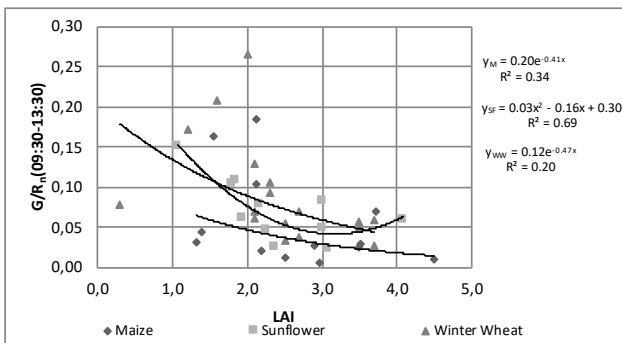


**Fig. 13.**  $G/R_n$ - LAI relationships for winter wheat, sunflower, and maize.

**Fig. 13.** Relazione tra  $G/R_n$ - LAI in frumento, girasole, e mais.

ly by collecting data samples, oven-dry them with  $65^{\circ}\text{C}$  heat and finally measuring the weight. Crop height data was also recorded periodically during the growing periods. There is an obvious negative relationship between  $G/R_n$  and crop height for each crop.  $G/R_n$  decreased with increasing crop height. The relationship is 2<sup>nd</sup> order polynomial for sunflower with an  $r^2$  value of 0.65, for maize, it is logarithmic with an  $r^2$  value of 0.58 and for winter wheat it is exponential with an  $r^2$  value of 0.57 (Fig. 12).

Again, with increasing LAI,  $G/R_n$  tended to decrease exponentially. However, this time  $r^2$  values were not much significant for winter wheat and maize (0.34 and 0.2) while for sunflower  $G/R_n$  seems to be defining LAI very well with 0.69  $r^2$  value (Fig. 13).

$G/R_n$  relationship with biomass found to be logarithmic for maize and sunflower and 2<sup>nd</sup> order polynomial for winter wheat with determination coefficients of 0.6, 0.56 and 0.5, respectively (Fig. 14). With growing vegetative mass  $G/R_n$  tended to decrease.

### 3.2 Relations between $G/R_n$ and SVIs

NDVI and SAVI increase up to 1.0 with growing vegetation. As  $G/R_n$  ratio linearly decreases with increasing vegetative cover, it is expected to have negative linear relations between  $G/R_n$  and NDVI and SAVI. Having a good understanding on the relationship between  $G$  and SVIs that could easily be obtained such as NDVI and SAVI allows acquiring an estimation for  $G$  which has a lot of uncertainty in measurements by depending on many parameters. There are several relationships in the literature in order to estimate  $G/R_n$  ratio. They either depend on crop's spectral properties (SVIs) or biophysical properties such as LAI and crop height. The ones with SVIs expressed to be either linear (Clothier *et al.*, 1986, Kustas and Daughtry, 1990), exponential (Jackson *et al.*, 1985, Singh *et al.*, 2008) or power function (Bastiaanssen *et al.*, 1998; Melesse and Nangia, 2005).  $G/R_n$  relationships with LAI, on the other hand, found to be exponential (Choudhury *et al.*, 1987; Kustas and Daughtry *et al.*, 1990).

Within this study, LAI and crop height's relationship to  $G/R_n$  were already demonstrated. NDVI and SAVI relationships for all three of the crops were shown at Fig. 15 and Fig. 16, respectively. There was no relationship obtained for winter wheat between NDVI and  $G/R_n$ , however for maize and sunflower, there were significant relationships with 0.73 and 0.63  $r^2$  values, respectively. The reason behind no relation detected between NDVI and  $G/R_n$  for winter wheat is most probably because most parts of the growing season were in winter. Since  $G$  is very sensitive to changes in weather conditions, soil wetness, and soil temperature, etc., the irrelevance can be explained by winter weather conditions.

SAVI and  $G/R_n$  were also in a good relationship for maize and sunflower with 0.70 and 0.61  $r^2$  values. There was a tiny improvement in  $r^2$  (0.23) value compared to

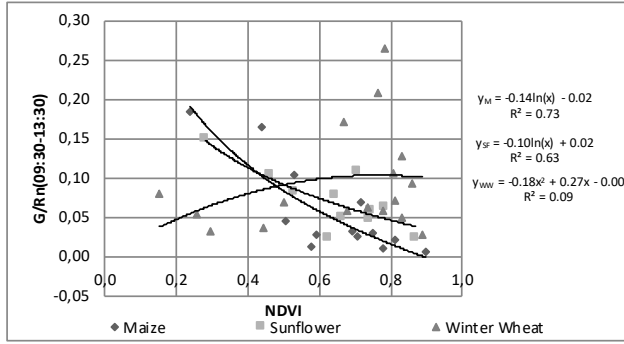


**Fig. 15.** NDVI-G/R<sub>n</sub> relationships for sunflower, maize and winter wheat.

**Fig. 15.** Relazioni tra NDVI-G/R<sub>n</sub> in girasole, mais e frumento.

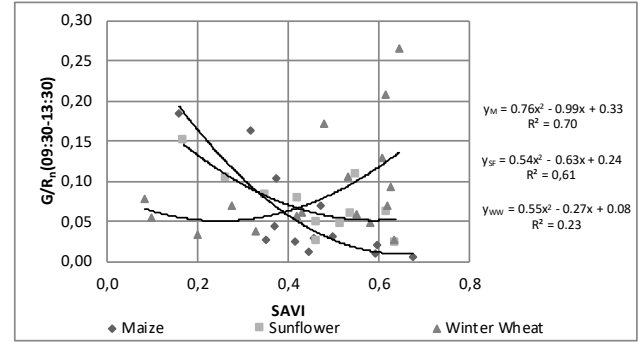


**Fig. 16.** SAVI-G/R<sub>n</sub> relationships for sunflower, maize and winter wheat.

**Fig. 16.** Relazioni tra SAVI-G/R<sub>n</sub> in girasole, mais e frumento.

the NDVI relationship for winter wheat that might be because of the soil adjustment parameter which SAVI included in its equation.

### 3.3 Assesment of Empirical Equations for G Estimation

Within the alignment of the knowledge obtained with above results, linear and nonlinear regression analysis carried out for determination of G/R<sub>n</sub>-SVIs/LAI/CH relationships referring to the models in Tab. 3. Equation 1-4 were the generalized versions of NDVI and SAVI based models in Tab. 3.

$$G = R_n * (Pr_1 * e^{(Pr_2 * NDVI)}) \quad (1)$$

$$G = R_n * (Pr_1 + Pr_2 * NDVI) \quad (2)$$

$$G = R_n * (Pr_1 * (1 - Pr_2 * (NDVI)^{Pr_5})) \quad (3)$$

$$G = R_n * (Pr_2 * (Pr_2 * SAVI - Pr_3) + Pr_4 * (1 - (Pr_2 * SAVI) - Pr_5)) \quad (4)$$

For LAI based relationships nonlinear regression analysis conducted considering the relation was exponential as shown in Equation 5. And finally crop height G/R<sub>n</sub> relationship was assumed to be exponential, power function and linear by using the models shown in Equation 6 and Equation 7.

$$G = R_n * (Pr_1 * e^{(Pr_2 * LAI)}) \quad (5)$$

$$G = R_n * (Pr_1 + Pr_2 * CH) \quad (6)$$

$$G = R_n * (Pr_1 * e^{(Pr_2 * CH)}) \quad (7)$$

**Tab. 3.** G estimation models used to evaluate in this study.

**Tab. 3.** Modelli di stima G usati in questo studio.

G Estimation Models	Ref
$G = R_n * (0.3811 * e^{(-2.3187 * NDVI)})$	Singh <i>et al.</i> , 2008
$G = R_n * (0.3 * (1 - 0.98 * NDVI^4))$	Bastiaanssen, 1998
$G = R_n * (-0.48 * NDVI + 0.46)$	Boegh <i>et al.</i> , 2004
$G = R_n * (0.1 * (1.62 * SAVI - 0.37)) + 0.5 * (1 - (1.62 * SAVI - 0.37))$	Boegh <i>et al.</i> , 2002
$G = R_n * (-0.49 * CH + 0.53)$	Payero <i>et al.</i> , 2005
$G = R_n * (0.34 * e^{(-0.46 * LAI)})$	Kustas <i>et al.</i> , 1993

Determination coefficients and RMS errors obtained with original G estimation models' parameters which are given in Tab. 3 and, with parameters suggested in this study are demonstrated for each and every crop and for each generalized model are shown in Table 4. Best results for each model and each crop are shown in bold writing.

According to the models' G predictions, overall the best result obtained with an exponential NDVI relationship (Singh *et al.*, 2008) with  $r^2$  equal to 0.831 and RMS error of 20.28 Wm<sup>-2</sup>. Although determination coefficient values for the Singh model were the best, lowest RMS errors monitored with parameters suggested in this particular study rather than with original ones. The best model for sunflower with respect to determination coefficient value, which was 0.751, was the LAI-based model (Kustas model); whereas for maize best model was an exponential NDVI-based model (Singh Model). For winter wheat on the other hand, generally, all models failed with the lowest determination coefficients and even with no relationships. Nonetheless, SAVI based model represented measured G's with  $r^2$  value as 0.744. Since most of the growing season of winter wheat is in cold weather conditions with heavy rain and snowfall, G might not be

**Tab. 4.** Results obtained with original parameters and, parameters suggested in this study together with determination coefficients and RMS errors for each crop.

**Tab. 4.** Risultati ottenuti con i parametri originali e i parametri suggeriti in questo studio insieme ai coefficienti di determinazione e gli errori RMS per ciascuna coltura.

Models	Crop Type		pr1	pr2	pr3	pr4	pr5	R <sup>2</sup>	RMSE
G = R <sub>n</sub> *(Pr <sub>1</sub> *(Pr <sub>2</sub> *SAVI-Pr <sub>3</sub> )+Pr <sub>4</sub> *(1-(Pr <sub>2</sub> *SAVI-Pr <sub>5</sub> )))	Sunflower	Boegh et al., 2002	0.100	1.620	-0.370	0.500	-0.370	0.709	119.430
		In this study	-0.373	0.436	0.212	0.075	0.125	0.668	13.892
	Maize	Boegh et al., 2002	0.100	1.620	-0.370	0.500	-0.370	0.735	140.804
		In this study	-0.330	0.905	0.431	0.072	0.083	0.688	19.784
	Winter Wheat	Boegh et al., 2002	0.100	1.620	-0.370	0.500	-0.370	0.162	142.795
		In this study	-0.430	-0.053	0.011	0.039	0.038	<b>0.744</b>	<b>9.933</b>
G=R <sub>n</sub> *(Pr <sub>1</sub> *e <sup>(Pr2*NDVI)</sup> )	Sunflower	Singh et al., 2008	0.381	-2.319	-	-	-	0.729	12.811
		In this study	0.270	-2.102	-	-	-	0.744	<b>9.933</b>
	Maize	Singh et al., 2008	0.381	-2.319	-	-	-	<b>0.831</b>	20.275
		In this study	0.442	-3.330	-	-	-	0.772	14.934
	Winter Wheat	Singh et al., 2008	0.381	-2.319	-	-	-	0.043	34.9648
		In this study	0.044	0.378	-	-	-	0.320	10.489
G= R <sub>n</sub> *(Pr <sub>1</sub> +(Pr <sub>2</sub> *NDVI))	Sunflower	Boegh et al., 2004	-0.480	0.460	-	-	-	0.706	38.592
		In this study	0.194	-0.185	-	-	-	0.746	<b>9.960</b>
	Maize	Boegh et al., 2004	-0.480	0.460	-	-	-	<b>0.791</b>	48.092
		In this study	0.242	-0.288	-	-	-	0.752	15.011
	Winter Wheat	Boegh et al., 2004	-0.480	0.460	-	-	-	0.038	65.573
		In this study	0.042	0.023	-	-	-	0.323	10.477
G=R <sub>n</sub> *(Pr <sub>1</sub> *(1-Pr <sub>2</sub> *(NDVI <sup>Pr3</sup> )))	Sunflower	Bastiaanssen, 1998	0.300	-0.980	4.000	-	-	0.739	66.969
		In this study	0.438	0.949	0.284	-	-	0.748	<b>10.443</b>
	Maize	Bastiaanssen, 1998	0.300	-0.980	4.000	-	-	0.596	81.578
		In this study	0.770	1.025	0.220	-	-	<b>0.775</b>	15.110
	Winter Wheat	Bastiaanssen, 1998	0.300	-0.980	4.000	-	-	0.018	75.201
		In this study	0.192	0.676	-0.081	-	-	0.327	10.863
G=R <sub>n</sub> *(Pr <sub>1</sub> *e <sup>(Pr2*LAI)</sup> )	Sunflower	Kustas et al., 1993	0.340	-0.460	-	-	-	0.684	24.087
		In this study	0.311	-0.689	-	-	-	<b>0.751</b>	9.906
	Maize	Kustas et al., 1993	0.340	-0.460	-	-	-	0.242	35.055
		In this study	0.144	-0.333	-	-	-	0.280	25.917
	Winter Wheat	Kustas et al., 1993	0.340	-0.460	-	-	-	0.216	20.525
		In this study	0.118	-0.262	-	-	-	0.314	<b>9.649</b>
G=R <sub>n</sub> *(Pr <sub>1</sub> +(Pr <sub>2</sub> *CH))	Sunflower	Payero et al., 2005	-0.490	0.530	-	-	-	<b>0.661</b>	112.588
		In this study	0.132	-0.050	-	-	-	0.625	11.898
	Maize	Payero et al., 2005	-0.490	0.530	-	-	-	0.395	313.530
		In this study	0.128	-0.034	-	-	-	0.516	20.920
	Winter Wheat	Payero et al., 2005	-0.490	0.530	-	-	-	0.276	57.916
		In this study	0.114	-0.079	-	-	-	0.429	<b>8.177</b>
G=R <sub>n</sub> *(Pr <sub>1</sub> *e <sup>(Pr2*CH)</sup> )	Sunflower	In this study	0.154	-0.702	-	-	-	<b>0.697</b>	10.782
	Maize	In this study	0.162	-0.614	-	-	-	0.556	20.013
	Winter Wheat	In this study	0.133	-1.227	-	-	-	0.426	<b>8.079</b>

estimated very well with other models but SAVI, since SAVI includes soil adjustment parameters. On the other hand, LAI based model worked fine for sunflower however for winter wheat and maize determination coefficients were low. For winter wheat, the reason behind these results might be the same why NDVI based models failed and, for maize the reason might be LAI values during both growing seasons were the highest. Finally, for crop height based G modelling, according to regression results it can be said that the model suggested in this study ( $G = R_n * (Pr_1 * e^{(Pr_2 * CH)})$ ) worked better than the one suggested by Payero *et al.* (2005) with greater  $r^2$  values together with lower RMS error values.

#### 4. DISCUSSIONS

In this study, energy fluxes measured over three different crop surfaces planted in the Thrace part of Turkey were examined to understand the seasonal and inter-annual variation of the  $G/R_n$  ratio by considering spectral and biophysical properties of vegetation together with soil dynamics, meteorological conditions, and land management activities. Among all the components necessary to compute evapotranspiration,  $R_n$  is the most crucial one, in terms of its important role in other physical and biological processes (Samani *et al.*, 2007). It stands for the difference between incoming and outgoing radiation at the earth surface and can be

used as a proxy data for climate change studies as well as agricultural meteorology (Bisht *et al.*, 2005). Measuring surface energy balance conventionally with direct methods represents only the point where the station is installed and a limited surrounding area. For regional studies locating the sensors properly and trying to determine how many installations needed are critical issues necessary to be considered carefully. Remote sensing techniques provide substantial opportunities to evaluate energy balance components over large areas. In the literature many researchers have tested remote sensing data together with atmospheric and land observations to estimate energy fluxes (Bastiaanssen *et al.*, 1998; Roerink *et al.*, 2000; Bisht *et al.*, 2005; Rimóczy-Paál, 2005; Silva *et al.*, 2005; Samani *et al.*, 2007; Di Pace *et al.*, 2008; Ryu *et al.*, 2008; Wang and Liang, 2009, Santos et al 2011). Obtained results in this study revealed that  $R_n$  and  $G$  can be estimated by remote sensing data with significantly good relationships. Having these relationships will improve the calibration of crop-climate growth models and therefore results in better estimations. However, to end up with a generalized result, it is crucial to continue collecting data over different soil-crop combinations for longer periods. Therefore, the knowledge of the energy fluxes' estimation for different vegetation cover-soil can be better represented by remote sensing data.

#### ACKNOWLEDGEMENT

We would like to thank Scientific and Technological Research Council of Turkey (TUBITAK) for supporting this research within the projects entitled as "Determination of Carbon Dioxide, Water Vapour and Energy Fluxes for Winter Wheat" (Project number: 109R006) and "Investigation of Possible Effects of Climate Change to Crop Growth by Crop Growth Models" (Project No: 108O567). We are thankful to Istanbul Technical University (ITU) for providing the opportunity. We would also like to thank Dr Fatih Bakanoğulları and all personnel who put their efforts collecting the data and managing the experimental field studies at Directorate of Atatürk Soil Water and Agricultural Meteorology Research Institute.

#### REFERENCES

- Allen, R., Irmak, A., Trezza, R., Hendrickx, J. M. H., Bastiaanssen, W., Kjaersgaard, J., 2011, Satellite-based ET estimation in agriculture using SEBAL and METRIC. *Hydrological Processes*, 25, 4011–4027.
- Baldocchi, D.B., Verma, S.B., Rosenberg, N.J., 1985, Water use efficiency in a soybean field: Influence of plant water stress. *Agric. For. Meteorol.* 34, 53–65.
- Basso, B., Ritchie, J. T., Pierce, F. J., Braga, R. , & Jones, J. W., 2001, Spatial validation of crop models for precision agriculture. *Agricultural Systems*, 68, 97–112.
- Bastiaanssen, W. G. M., Pelgrum, H., Wang, J., Ma, Y., Moreno, J. F., Roerink, G. J., Van der, W. T., 1998, A Surface Energy Balance Algorithm for Land (SEBAL) 1. Formulation. *J. Hydrol.*, 212, 198–212.
- Bastiaanssen, W.G.M., 1995, Regionalization of surface flux densities and moisture indicators in composite terrain, Theses (PhD), Wageningen Agricultural University, Wageningen, Netherlands, 273f.
- Bisht G., V. Venturini, S. Islam and L. Jiang, 2005. Estimation of the net radiation using MODIS (Moderate Resolution Imaging Spectroradiometer) data for clear sky days. *Remote Sens. Environ.* 97, 52–67.
- Boegh, E., Soegaard, H., Thomsen, A., 2002, Evaluating evapotranspiration rates and surface conditions using Landsat TM to estimate atmospheric resistance and surface resistance. *Remote Sens. Environ.*, 79, 329–343.
- Boegh, E., Soegaard, H., Christensen, J. H., Hasager, C. B., Jensen, N. O., Nielsen, N. W., 2004, Combining weather prediction and remote sensing data for the calculation of evapotranspiration rates: application to Denmark. *Int. J. Remote Sens.*, 25, 2553–2574.
- Choudhury, B.J., Idso, S.B., Reginato, J.R., 1987, Analysis of an empirical model for soil heat flux under a growing wheat crop for estimating evaporation by an infrared-temperature based energy balance equation. *Agric. For. Meteorol.* 39, 283–297.
- Clothier, B. E., Clawson, K. L., Pinter, Jr. J., Moran, M. S., Reginato, R. J., Jackson R. D., 1986, Estimation of soil heat flux from net radiation during the growth of alfalfa. *Agric. For. Meteorol.*, 37, 319–329.
- Camuffo, D., Bernardi, A., 1982, An observational study of heat fluxes and their relationships with net radiation. *Boundary-Layer Meteorology* 23(3), 359–368.
- Di Pace F. T., B. B. Silva, V. R. Silva and S. T. A. Silva, 2008. Mapeamento do saldo de radiação com imagens Landsat 5 e modelo de elevação digital. *Revista Bras. Engenharia Agrícola e Ambiental* 12, 385–392.
- Domingo, F., Villagarcia, L., Benner, A.J., Puigdefabregas, J., 2000, Measuring and modeling the radiation balance of heterogeneous shrubland. *Plant and Cell Environment* 23(1), 27–38.
- Dugas, W. A., R. A. Hicks, Gibbens, R. ,1996. Structure and functions of C3 and C4 Chihuahuan Desert plant communities: Energy balance components. *J. Arid Environ.* 34, 63–79.

- FAO, 2014, Food and agricultural organization of united nations, FAOSTAT, Data. Available at: <http://www.fao.org/faostat/en/#data>. Accessed on 15 July 2017.
- Hsieh, C. I., Huang, C. W., Kiely, G., 2009, "Long-term estimation of soil heat flux by single layer soil temperature, *International Journal Of Biometeorology*, 53, 113-123.
- Huete, A.R., 1988, A soil-adjusted vegetation index (SAVI). *Remote Sensing of Environment*, 25, 3, 295 – 309.
- Idso SB, Aase JK, Jackson RD, 1975, Net radiation–soil heat flux relations as influenced by water content variations. *Boundary-Layer Meteorology*, 9, 113–122.
- Jackson, R.D., Pinter, J., Jr., Reginato, R.J., 1985, Net radiation calculated from remote multispectral and ground station meteorological data. *Agric. For. Meteorol.*, 35, 153-164.
- Kumar, K. K., and Rao V. U., 1984, Significance of soil heat flux in the estimation of potential evapotranspiration. *Indian J. of Ecology* 11, 68-70.
- Kustas, W. , Choudhury, B. J., Moran, M. S., Reginato, R. J., Jackson, R. D., and Gay, I. W., 1987, Problems in the estimation of sensible heat flux over incomplete canopy cover with thermal infrared data. In: 18th Conference of Agricultural and Forest Meteorology and 8th Conference on Biometeorology and Aerobiology, Purdue University, 87-90.
- Kustas, W. , Daughtry, C. S. T., Oevelen, J. V., 1993, "Analytical treatment of relationships between soil heat flux/ net radiation ratio and vegetation indices", *Remote Sensing of Environment*, 46, 319 – 330.
- Kustas, W. , and C. S. T. Daughtry, 1990: Estimation of the soil heat flux/net radiation ratio from spectral data. *Agric. For. Meteorol.*, 49, 205–233.
- Kustas, W. , Prueger, J. H., Hatfield, J. L., Ramalingam, K., Hipps L. E., 2000, Variability in soil heat flux from a mesquite dune site. *Agric. Forest Meteorol.* 103, 249-264.
- Melesse, A. M., and Nangia, V., 2005, Estimation of spatially distributed surface energy fluxes using remotely sensed data for agricultural fields. *Hydrol. Proc.* 19, 2653-2670.
- Murray, T., and Verhoef, A., 2007a. Moving towards a more mechanistic approach in the determination of soil heat flux from remote measurements: I. A universal approach to calculate thermal inertia. *Agric. Forest Meteorol.* 147, 80-87.
- Murray, T., and Verhoef, A., 2007b. Moving towards a more mechanistic approach in the determination of soil heat flux from remote measurements: II. The diurnal shape of soil heat flux. *Agric. Forest Meteorol.* 147, 88-97.
- Novak, M. D., 1993, Analytical solutions for two-dimensional soil heat flow with radiation surface boundary conditions. *Soil Science Society of America J.* 57(1), 30-39.
- Núñez, C. M., Varas, E. A., Meza, F. J., 2010, Modeling soil heat flux. *Theoretical Applied Climatology*, 100, 251-260.
- Ogee, J., Lamaud, E., Brunet, Y., Berbigier, , Bonnefond, J. M., 2001, A long-term study of soil heat flux under a forest canopy. *Agricultural Forest Meteorology.*, 106, 173–186.
- Ohmura, A., 1982. Objective criteria for rejecting data for Bowen ratio flux calculations. *J. Appl. Meteorol.* 21, 595–598.
- Parker, D. C., and Wolff, M. F., 1965, Remote Sensing. *International Science and Technology*, 43, 20-31.
- Payero, J. O., Neale, C. M. U., Wright, J. L., Allen, R. G., 2003, Guidelines for validating Bowen ratio data. *Transactions of the ASAE* 46, 1051-1060.
- Payero, J., Neale, C., Wright, J., 2005, Estimating soil heat flux for alfalfa and clipped tall fescue grass. *Applied Engineering in Agriculture, American Society of Agricultural Engineers*, v.21, n.3, 401-409.
- Perez, J., F. Castellvi, M. Ibañez, J.I. Rosell, 1999. Assessment of reliability of the Bowen ratio method for partitioning fluxes, *Agricultural and Forest Meteorology*, 97, 141-150.
- Rimóczi-Paál A., 2005. Mapping of radiation balance components for the region of Hungary using satellite information. *Phys. Chem. Earth* 30, 151-158.
- Roerink G. J., Z. Su and M. Menenti, 2000. S-SEBI: A Roerink G. J., Su Z., Menenti M., 2000, S-SEBI: A Simple Remote Sensing Algorithm to Estimate the Surface Energy Balance, *Phys. Chem. Earth (B)*, Vol. 25, No. 2, pp. 147-157.
- Rouse, J. W., Haas, R. H., Schell, J. A., Deering, D. W., and Harlan, J. C., 1974, "Monitoring the vernal advancement and retrogradation (green-wave effect) of natural vegetation," *\_NASA/GSFC Type III Final Report\_*, Greenbelt.
- Ryu Y., S. Kang, S. Moona and J. Kim, 2008. Evaluation of land surface radiation balance derived from moderate resolution imaging spectroradiometer (MODIS) over complex terrain and heterogeneous landscape on clear sky days. *Agr. Forest Meteorol.* 148, 1538-1552.
- Santos C. A. C. D., Nascimento R. L. D., Rao T. V. R. Manzi, A. O., 2011, Net radiation estimation under pasture and forest in Rondônia, Brazil, with TM Landsat 5 images, *Atmosfera* 24 (4) pp.435-446
- Samani Z., Bawazir A. S., Bleiweiss M., Skaggs R., Tran V.D., 2007, Estimating Daily Net Radiation over

- Vegetation Canopy through Remote Sensing and Climatic Data, *Journal Of Irrigation And Drainage Engineering*, DOI: 10.1061/\_ASCE\_0733-9437\_2007\_133:4\_291
- Silva B. B., G. M. Lopes, and V. Azevedo, 2005. Balanço de radiação em áreas irrigadas utilizando imagens Landsat 5 – TM. *Rev. Bras. Meteor.* 20, 243-252.
- Singh, R. K., Irmak, A., Irmak, S., Martin D. L., 2008, Application of SEBAL model for mapping evapotranspiration and estimating surface energy fluxes in south-central Nebraska. *J. Irrig. Drain. Eng.* 134, 273-285.
- Stroppiana, D., Boschetti, M., Brivio, A., Bocchi, S., 2006, Remotely sensed estimation of rice nitrogen concentration for forcing crop growth models, *Italian Journal of Agrometeorology* 3, 50-57.
- Şaylan, L., Bakanoğulları, F., Çaldağ, B., Çaylak, O., Özkoca, Y., Semizoğlu, E., Karayusufoğlu S. 2010. Investigation of the possible impacts of climate change to crop growth by crop growth models, I. National Soil and Water Resources Congress, 1-4 June, Eskisehir, Turkey.
- Şaylan, L., Semizoğlu Ceyhan, E., Bakanoğulları, F., Çaldağ, B., Özkoca, Y., Karayusufoğlu Uysal, S., Altınbaş, N., Eitzinger, J., 2018. Analysis of Seasonal Carbon Dioxide Exchange of Winter Wheat Using Eddy Covariance Method in the Northwest Part of Turkey, *Italian Journal of Agrometeorology* 3, 39-52.
- Tasumi, M., 2003, Progress in operational estimation of regional evapotranspiration using satellite imagery. Ph. D. Dissertation, University of Idaho, Moscow, Idaho.
- TSMS, 2000, Turkish state meteorological service, Climate classification. Available at: <https://mgm.gov.tr/iklim/iklim-siniflandirmalari.aspx?m=KIRKLARELI>. Accessed on 10 July 2017.
- TSMS, 2016, Turkish state meteorological service, City-based assessment, Available at <https://mgm.gov.tr/veridegerlendirme/il-ve-ilceler-istatistik.aspx?m=KIRKLARELI>. Accessed on 27 July 2017.
- TUIK, Turkish statistical institute, 2016, Agricultural production statistical tables, Available at [http://www.turkstat.gov.tr/PreTablo.do?alt\\_id=1001](http://www.turkstat.gov.tr/PreTablo.do?alt_id=1001). Accessed on 15 July 2017.
- Tukey, J. W., 1977, *Exploratory data analysis*. Addison-Wesely.
- Van der Tol, C., 2012: Validation of remote sensing of bare soil ground heat flux. *Remote Sensing Environment*, 121, 275-286.
- Verhoef, A., 2004, Remote estimation of thermal inertia and soil heat flux for bare soil. *Agric.For.Meteor.*, 123, 221-236.
- Verhoef, A., Ottlé, C., Cappelaeere, B., Murray, T., Saux-Picart, S., Zribi, M., Maignan, F., Boulain, N., Demarty, J., Ramier, D., 2012, Spatio-temporal surface soil heat flux estimates from satellite data; results for the AMMA experiment at the Fakara (Niger) supersite. *Agricultural Forest Meteor.*, 154, 55-66.
- Wang, J., and Bras, R.L., 1999, Ground heat flux estimated from surface soil temperature. *Journal of Hydrology*, 216, 214-226.
- Wang W. and S. Liang, 2009. Estimation of high-spatial-resolution clear-sky longwave downward and net radiation over land surfaces from MODIS data. *Remote Sens. Environ.* 113, 745-754.